OPEN ACCESS

University of BRISTOL

Chekkal, I., Cheung, R. C. M., Wales, C., Cooper, J. E., Allen, N. J., Lawson, S., Peace, A. J., Cook, R., Standen, P., Hancock, S. D., & Carossa, G. M. (2014). Design of a Morphing Wing-tip. In *22nd AIAA/ASME/AHS Adaptive Structures Conference* [1262] American Institute of Aeronautics and Astronautics Inc. (AIAA). https://doi.org/10.2514/6.2014-1262

Peer reviewed version

Link to published version (if available):
10.2514/6.2014-1262

Link to publication record in Explore Bristol Research
PDF-document

Copyright © 2014 by the American Institute of Aeronautics and Astronautics, Inc. All rights reserved.

University of Bristol - Explore Bristol Research
General rights

This document is made available in accordance with publisher policies. Please cite only the published version using the reference above. Full terms of use are available:
http://www.bristol.ac.uk/red/research-policy/pure/user-guides/ebr-terms/

Design of a Morphing Wing-tip

J. E. Cooper[1], I. Chekkal[2], R. C. M. Cheung[3] & C. Wales[4]
University of Bristol, Bristol, BS8 1TH, UK.

N. J. Allen[5], S. Lawson[6] & A. J. Peace[7]
Aircraft Research Association Ltd, Manton Lane, Bedford, MK41 7PF, UK.

R. Cook[8], P. Standen[9] & S. D. Hancock[10]
Stirling Dynamics Ltd, 26 Regent Street, Clifton, Bristol, BS8 4HG, UK.

G.M. Carossa[11]
Alenia Aermacchi, C.so Francia 426, 10146 Torino, Italy

An initial design of a morphing wing-tip for a Regional Jet aircraft is developed and evaluated. The adaptive wing-tip concept is based upon a chiral type internal structure, enabling controlled cant angle orientation, camber and twist throughout the flight envelope. A baseline Turbo-Fan Aircraft configuration model is used as the benchmark to assess the device. CFD based aerodynamics are used to evaluate the required design configurations for the device at different points across the flight envelope in terms of lift/drag and bending moment distribution along the span, complemented by panel method based gust load computations. Detailed studies are performed to show how the chiral structure can facilitate the required shape changes in twist, camber and cant. Actuator requirements and limitations are assessed, along with an evaluation of the aerodynamic gains from the inclusion of the device versus power and weight penalties. For a typical mission it was found that savings of around 2% in fuel weight are possible using the morphing wing-tip device. A similar reduction in weight due to passive gust loads alleviation is also possible with a slight change of configuration.

---

[1] Royal Academy of Engineering Airbus Sir George White Professor of Aerospace Engineering. AFAIAA
[2] Research Assistant, Dept of Aerospace Engineering
[3] Research Assistant, Dept of Aerospace Engineering
[4] Research Assistant, Dept of Aerospace Engineering
[5] Senior Project Scientist, Computational Aerodynamics
[6] Senior Project Scientist, Computational Aerodynamics
[7] Chief Scientist, Computational Aerodynamics
[8] Engineer, Aerospace Engineering
[9] Technical Manager, Aerospace Engineering
[10] Research and Development Manager
[11] Section Leader, Structural Loads, Air Vehicle Technology,

Nomenclature

f	Specific fuel consumption
g	Acceleration due to gravity
y	Distance from neutral axis
C_L, C_{LL}	Total and local lift coefficients
C_D, $C_{D'}$	Total and parasitic drag coefficients
C_{ML}, C_{YL}, C_{NL}	Local pitching moment, side force and normal force coefficients
C_M, C_{DP}, C_{DF}	Pitching moment, pressure drag and skin friction drag coefficients
I	2nd moment of area
M	Bending moment
R	Range
S_{FM}	Fuel mass ratio
V	Airspeed
W_1, W_2	Take-off and landing weight

I. Introduction

Despite the recent effects of terrorism, health scares, international conflicts and volcanos, the aerospace sector is expected to increase at an average 4-5% p.a. over the next few decades, significantly above global GDP growth; in air transport terms, this implies a doubling of traffic about every 16 years[1,2]. It is evident that environmental requirements, such as emissions and noise, will play a dominant role in future transport aircraft development, becoming a driving force for aircraft design. These are the underlying reasons for which ACARE, in the 20-20 Vision and FlightPath2050 initiatives[1,2], established the so-called *greening of aircraft* as a prime objective for future research activities related to Aeronautics.

The green design criteria, as formulated in the FlightPath2050 Agenda, are represented by: 90% cut in NO_x emissions; 65% perceived aircraft noise levels and a 75% cut in CO_2 emissions per pass-Km, all compared to the overall levels in 2000. The classic Breguet range equation tells us that the only ways of achieving these goals are through better engines, more aerodynamically efficient wings, and lighter structures. However, traditional aircraft design only optimizes to a single point in the flight envelope and fuel condition, and therefore all aircraft are sub-optimal at every other point in the flight envelope. It is likely that more efficient aircraft, able to meet direct and indirect environmental requirements, will be achievable only by enhancing the aircraft's capability through adapting

its configuration in-flight, so as to be always in the optimal configuration. Such an approach is usually referred to as "morphing"[3], and Barbarino et al.[4] review some of the advantages and drawbacks of various morphing approaches.

From a practical point of view, it is commonly accepted that morphing can be categorized into "local morphing" (where the change in configuration is limited only to some part of aircraft) and "global morphing" (where global aircraft characteristics such as wingspan, planform, sweep angle, are changed) disciplines. One of the most notable global morphing aircraft concepts was the NextGen aircraft[3] which enabled dramatic planform changes in a UAV structure; however, this was achieved using polymer type skins, which are not envisaged to be feasible for commercial jet aircraft.

There has been much morphing research over the past 15 years, including the Active Flexible Wing[5], Active Aeroelastic Wing[6], 3AS[7], SMorph[8], SADE[9] and NOVEMOR projects. Much of this activity has investigated different morphing concepts, but this has been rather haphazard and there is no clear way to determine which is the best concept. Most of the concepts have been applied to either small wind tunnel models or UAVs, in particular to structures that do not have stressed skins, including work focused upon the use of morphing wing-tips[10-14] (sometimes referred to as Morphlets). Much less effort has been employed on to the use of morphing structures that enable loads alleviation, such as that developed in the SMorph project[8] which achieved a 22% mass reduction in a sensorcraft structure for some configurations[15,16]. Gust and maneuver loads are often the key design cases for civil aircraft, and if the device is able to reduce the gust loading, then this can be transformed into a mass reduction, thus saving fuel requirements in addition to the benefits of the drag reductions achieved through aerodynamic shape change. Finally, chiral structures have also received some attention in recent years, initially as a means to achieve zero Poisson's Ratio structures, but there have been few attempts to employ them to morph wing type structures[17-19].

In this paper, work undertaken as part of the EU Clean Sky CLAReT (Control and Alleviation of Loads in Advanced Regional Turbo-Fan Configurations) project is described. A novel adaptive wing-tip concept is developed, based upon a chiral type internal structure, enabling controlled cant angle orientation, camber and twist throughout the flight envelope, whilst also providing a passive gust loads alleviation capability. Figure 1 shows a road-map of the project and highlights the aerodynamic, morphing structure, actuation and assessment phases that were considered. A baseline Turbo-Fan Aircraft configuration model was used as the benchmark to assess the device. Aerodynamic requirements were defined through investigation of the required configurations (twist, camber and cant) at different points in the flight envelope (M = 0.48, 0.60 and 0.74) in terms of lift/drag and bending moment distribution along

the span, along with panel method based gust load computations. It is shown how a chiral structure (a repeating structure whose components are not equal to their reflection and often possessing a negative Poisson's ratio characteristic) can facilitate the required shape changes, followed by an assessment of the actuator, system and requirements. A comparison of performance gains through the use of the morphing device is made with the baseline "traditional" design, along with an overall evaluation of the pros and cons of using such a device. Further studies demonstrate the use of the device for passive gust alleviation which can lead to further weight reduction.

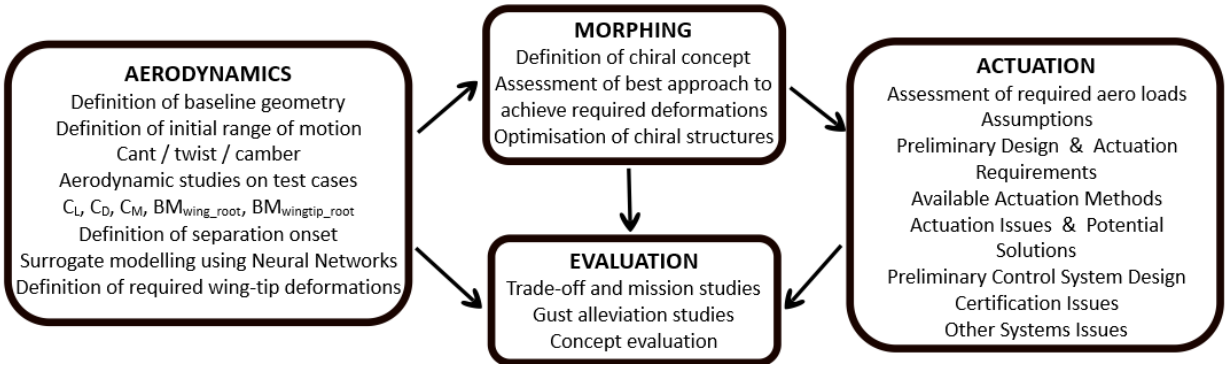

Figure 1. CLAReT Roadmap

II. Flexible Wing-tip Model

The underlying model for these studies was a regional jet with aspect ratio of 10.5 and wing sweep 25°. The baseline wing-tip, shown in Figure 2, was produced by extending the original wing (of length 18.78m from wing root to tip) used in this study by 1.5m, with a cant of 50° and taper ratio 0.4. A blend region was used in order to reduce the effect of the junction between the wing and wing-tip. To reduce the shock strength, and thus the tendency for shock induced separation at high AoA design cruise (Mach 0.74) cases, the thickness to chord ratio was reduced by 25% and the leading edge sweep increased in the blend region. In addition the wing-tip chord was also reduced by 25% through the blend region. Aerodynamic analysis was performed using the viscous-coupled VCFlite3D code in order to determine the aerodynamic loads (and resulting bending moments) across the wing and wing-tip. This type of CFD methodology (Euler + boundary layer) is much faster than RANS and hence more appropriate for generating large databases.

The wing-tip design was parameterized in terms of cant angle, twist and camber profile. The effect of changing these parameters on aerodynamic performance, wing-tip root and wing root bending moment was evaluated. These

analyses were performed for a range of angles of attack and Mach numbers, as shown in Table 1. It is assumed that there is a perfect change of shape in the blend region.

Figure 2 Baseline Wing-tip Design and Cant Angles Considered.

Positive cant was defined as the angle between the straight line representing the continuation of the wing and the plane of the wing-tip. Cant angles of 0°, 25°, 50° and 90° were used to assess the effect of the variation of this parameter. The effects of the cant angle on the drag, shown in Figure 3, appear to be small as plotted here; however, it should be noted that these differences amount to several drag counts (up to 6%), which would have a significant effect on fuel consumption over the life of the aircraft. The drag values include friction drag which adds around 0.005 to the overall drag coefficient. It was found that there was a strengthening normal shock in the blend region as the cant angle increased, which also has an influence on the wing-tip, as shown in Figure 4. With higher cant angles, VCFlite3D failed to give a solution for higher incidence angles, a result of significant flow separation in the blend region, which can cause the boundary layer package to fail, and this was viewed as approximately marking the extent of the attached flow regime.

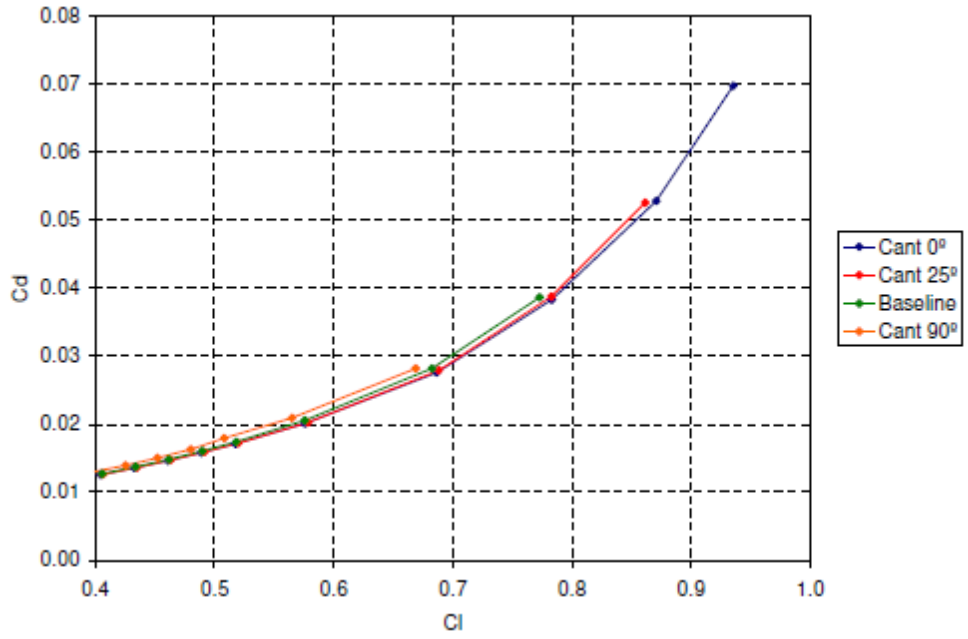

Figure 3 Drag Polars For Different Cant angles on at Mach 0.74

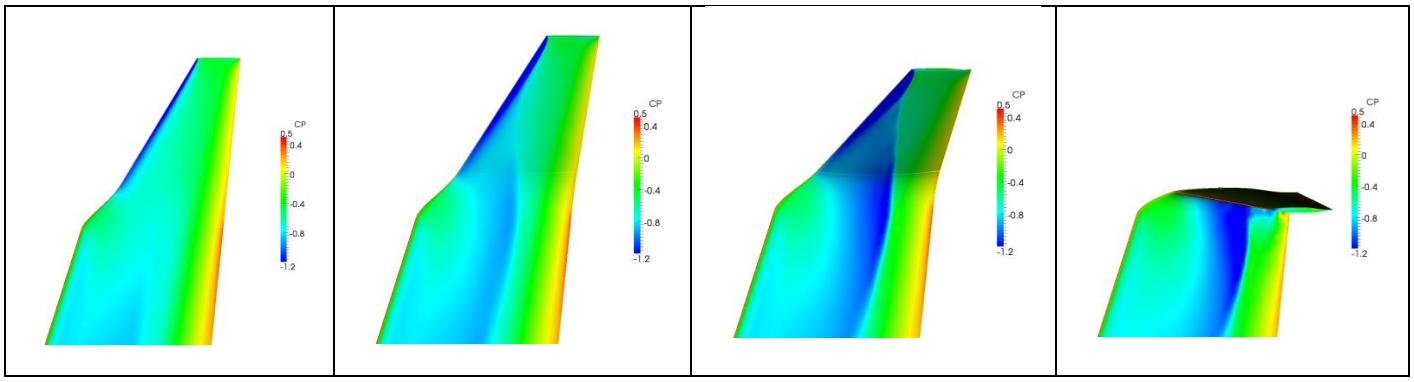

Figure 4 Pressure contours for Cant Angle of 0°, 25°, 50° and 90°, Mach 0.74, α = 0.5°

	M	AoA(º)	Cant(º)	Twist(º)	Camber
Range	**[0.48, 0.60, 0.74]**	**-0.5 →3**	**0 → 70**	**-5 → 5**	**0.75 → 2**

Table 1 Input Parameters Considered

Twist was defined around the quarter chord position, with positive twist being a toe-in angle. The effect of the twist angle on drag appears to be smaller than that for the cant angle, as shown in Figure 5. At higher incidences the negative twist angle helps reduce the shock strength substantially; which is why it is possible to achieve a higher C_L without separation for negative wing-tip twist.

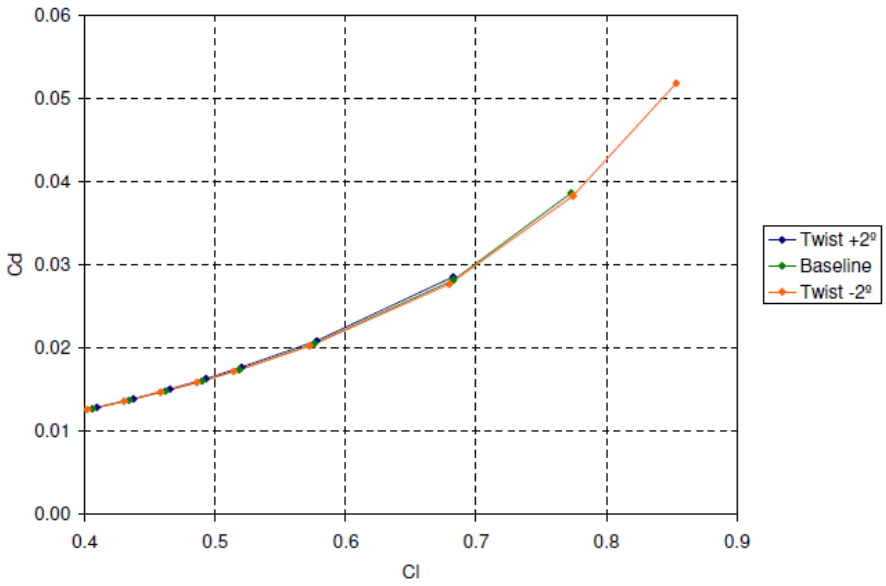

Figure 5 Effect of twist on drag at Mach 0.74

Changes to the camber were defined as a factor, representing a deviation from the baseline camber line. The distance of the baseline camber line from the chord line was known for each point along the chord, and this distance was multiplied by a factor to obtain a new geometry. A factor of two implies that the distance from the camber line to the chord line at each point along the chord is double that of the baseline wing-tip, as shown in Figure 6. An airfoil with no camber would have a factor of zero. Variations of the camber factor of 0.75, 1.25 and 2.0 were initially considered.

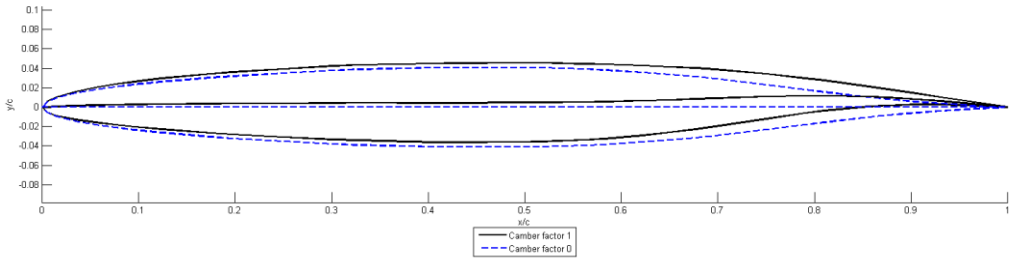

Figure 6 Camber factor of zero (dashed); baseline camber factor of one (solid)

Figure 7 shows that camber factor has very little effect on the total drag; however, small changes in the pressure distribution on the wing-tip close to the trailing edge occur at the highest camber factor of 2.0.

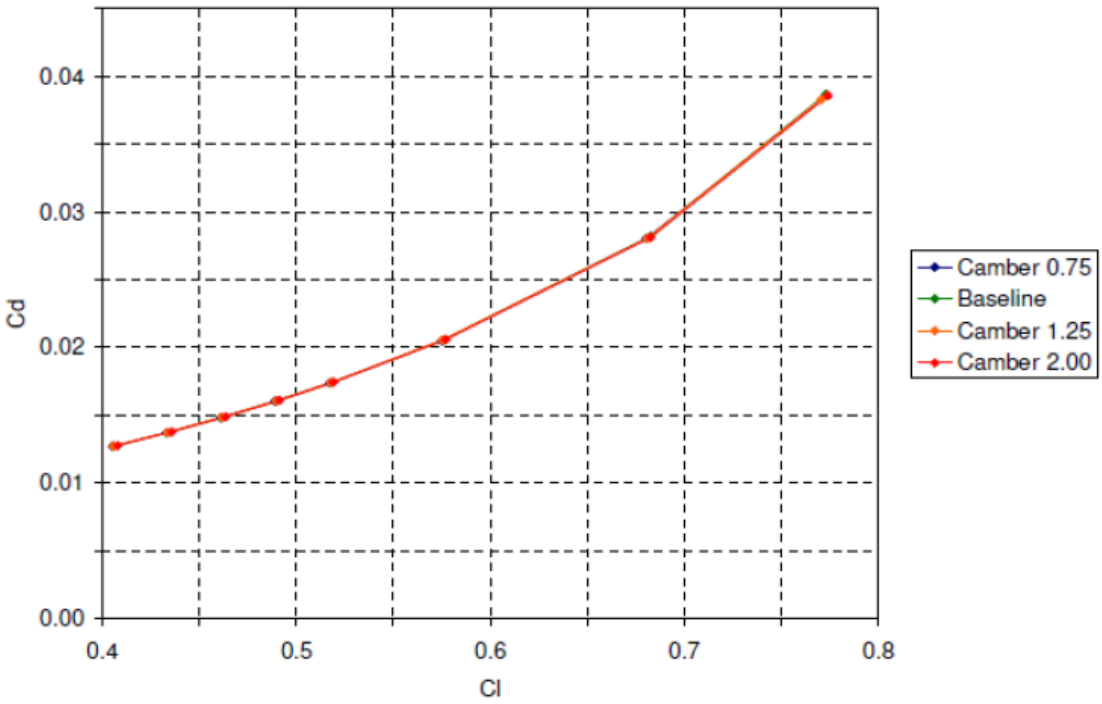

Figure 7 Effect of camber factor on drag at Mach 0.74

To ensure the computation required for the aerodynamic calculations is performed efficiently, a database of 48 geometries with varying cant, camber and twist values was generated using a Latin Hypercube sampling approach to ensure a thorough distribution across the design space. A range of aerodynamic parameters were calculated for each of the cases shown in Figure 8. Multilayer feed-forward neural networks were trained using the 48 geometries. These neural networks were used to investigate the sensitivity of aerodynamic properties, as well as wing and wing-tip

bending moments, to variations in cant, twist and camber for a range of Mach number (M) and angle of attack (AoA) as seen in Table 2 where it can be deduced that there is no single best orientation; what is good from the aerodynamic viewpoint is not good from the structural (bending / pitching moment) viewpoint. From the neural network model, the best 10 configurations (Table 3) were found for different objectives to identify important regions of the parameter space. It was found that the cant and twist angles had more effect on C_L/C_D, the wing root bending moment (WRBM) and wing-tip root bending moment (WTBM) than camber, whereas twist had more effect on the pitching moment C_m than the camber and cant. These findings reduced the range of motion that was required for the wing-tip deflections.

III. Morphing Concept

The adaptive wing-tip is required to be able to achieve the desired target cant, twist and camber deflections. In this work, a hexagonal chiral structure was employed, the geometry of which depends upon the L, R and r topological parameters, as defined in Figure 9. In particular, the parameter ratio L/R (ratio of side of triangles to distance between center of hexagons) has a significant effect on the deflection behavior of the chiral structure. Noting that, due to anisotropy, chiral structures in 3D can have a preferred direction of deformation, it was proposed to split the wing-tip into two regions to provide span-wise and chord-wise deflections with the chiral structure oriented at 90° to each other, using the layout shown in Figure 10. In the proposed design, the chiral structure is positioned to produce changes in cant in the blend region, whilst it is oriented to produce changes in twist and camber through the rest of the wing-tip geometry. The chiral structure can be deformed by either rotating the nodes or bending of the ligaments as seen in Figure 9. Here, rotation of the nodes was used as the deformation mechanism to achieve the desired cant, twist and camber deflections via the use of torsional actuation.

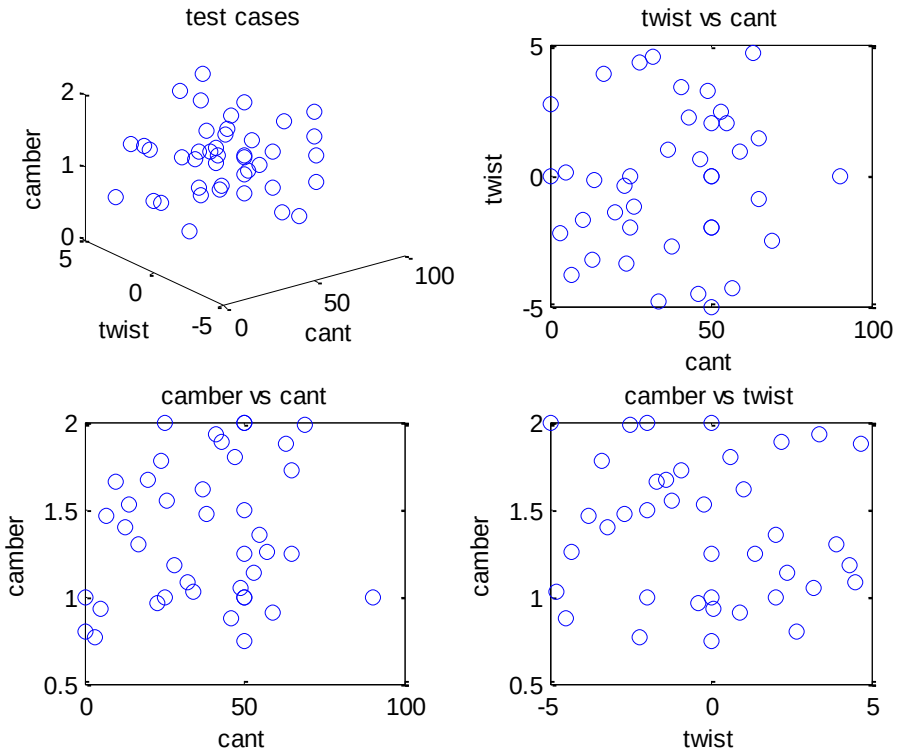

Figure 8 Test Cases Used for Generation of Aerodynamic Database

	Cant (°)	Twist (°)	Camber Factor
C_L/C_D (highest)	0 → 10	-5 → 2	1.25 → 2.00
C_M (lowest)	30 → 70	-5 → -1	0.75
WRBM (lowest)	0 → 70	-5 → 5	0.75
WTBM (lowest)	50 → 70	-5 → 5	0.75

Table 2 Ranges of best morphing parameters for different objectives.

Geometry	Cant (°)	Twist (°)	Camber Factor
3 (Baseline)	50	0.0	1.00
4	90	0.0	1.00
11	25	-2.0	2.00
12	50	-5.0	2.00
21	10	-1.7	1.66
22	32	4.5	1.08
31	53	2.4	1.14
43	77.5	-1.7	0.60
44	20	-3.5	0.50
45	85	-4.0	1.70
48	75	-4.5	1.50

Table 3 Wing-tip orientations used in loads study

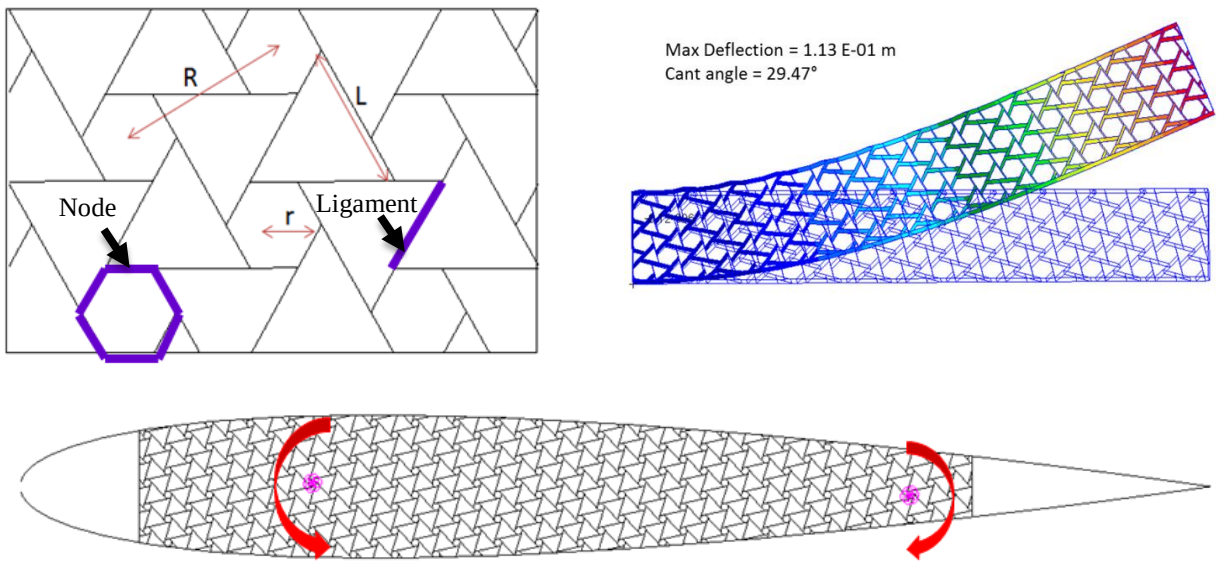

Figure 9 Chiral structure parameters and actuation options

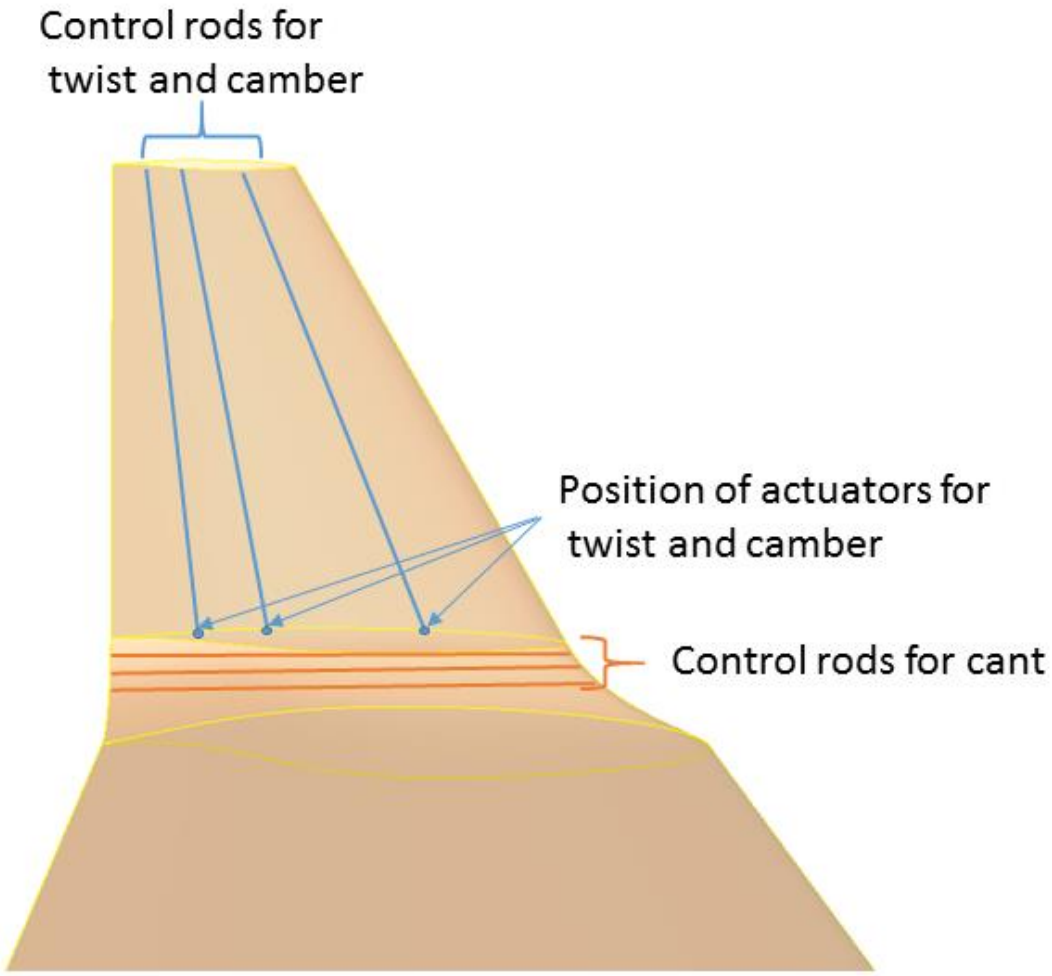

Figure 10 Actuator position and chiral orientation

The material used in the model was a 6000 series aluminum alloy (Young's modulus E = 69GPa, density $\rho = 2700$ kg/m^3, and Poisson's ratio $\nu = 0.33$). This material was used for the front and rear spars, as well as for the chiral structure inside the wing box. The core structure has a wall thickness of t = 0.76mm. When varying the camber shape, most of the shape change occurs towards the rear of the airfoil, therefore the leading edge region can be assumed to be stiffer and the same material is used for the skin forward of the front spar. The trailing edge region is very thin with little room for any chiral structure; hence, the trailing edge region behind the rear spar is also made of the same aluminum. The skin between the two spars needs to be softer to allow the structure to morph[19].

Therefore, for the outer skin over the wing box, an aluminum alloy with lower stiffness properties[20] was used to facilitate the desired bending deformations (Young's modulus E = 9 GPa, density $\rho = 2700$ kg/m^3, and Poisson's ratio $\nu = 0.33$), again with a wall thickness of t = 0.76mm. The choice of skin for morphing applications is still an open issue[21].

An optimization study was performed to determine the best configuration of the chiral structure, investigating the effect of varying the L/R ratio within the range [0.60-0.95] on the amount of achievable deflection and smoothness of outer skin. It was found that a core design of L/R = 0.87 generated high deflections for a given actuator loading, whilst maintaining a smooth outer skin for aerodynamic efficiency.

The cant actuators were positioned at the outboard end of the blend region to lower the actuation requirements. For actuators placed further inboard, the deflections are constrained by the stiffness of the wing-tip. For twist, the actuator is placed at the quarter chord point of the wing-tip, and this actuator is also used in conjunction with two rear actuators in order to produce the required change in camber. Using this base line structure and actuator positioning, the torque that each actuator has to produce to achieve the required parameter changes could be determined. Note that there is no need to produce a cant change of 90^o but, by deflecting $\pm 45^o$ about the mean cant angle, it is possible to achieve the required range of cant angles without excessive skin strains.

IV. Actuation

The aim of the morphing wing-tip is to achieve the optimal configuration at different flight phases in an adaptive manner and as a result of this requirement, high speed action is not required. Defining an actuation system to deliver the required torque within the available space specified in the proposed wing-tip design is a challenging task, due to the very thin section of the wing-tip (and nearby region) and the large torques required.

A number of candidate devices for achieving these levels of torque within the allowable volumes have been considered and a market survey carried out into the currently available capabilities of each these devices.

Various types of actuators which are driven using hydraulic and/or electric power are available, each with their own advantages and limitations. Stepper-motors and servo-motors provide simple angular-position control but are not well suited for the relatively high-torques required here. Vane actuators (which use differential fluid pressure either side of an asymmetric rotating vane to provide torque) can provide higher torques, but are generally too large (and heavy) for consideration for this use. A suitably sized electric motor/actuator would probably provide a lower torque

(and a higher speed) than is required, although it may perhaps be possible to overcome this problem by fitting it on the inner wing or fuselage, and delivering the (increased) torque to the controlling rod by a gear train or similar mechanism. This would, however, introduce significant extra mass and complexity (hence increasing inspection and maintenance needs), and so was not considered further here. Rack & pinion actuators (which use a toothed rod and wheel to transform linear force to torque) can, however, provide fairly high torques from relatively small actuators. From consideration of a number of different actuator types and power sources, hydraulic rack & pinion actuators offer the closest match to the desired capabilities for controlling the wing-tip, in terms of torque produced and actuator size.

Due to the tight space requirements, it is not possible to fit the required actuators for cant as well as the camber and twist actuators. Whilst it is not possible to meet fully the actuation needs for any of the degrees of freedom within the available spaces, there is only a small deficit in the capabilities and sizes for the cant actuation needs. For the twist & camber actuators, it is not possible to obtain even a significant fraction of the required torque using actuators located at the desired positions, at the base of the wing-tip. It may, however, be possible to install more powerful actuators on the inboard wing section, where the available volume is greater. This would require means of transferring the torque produced here to the base of the wing-tip.

With current levels of actuator power available in the space (as of August 2013), it is possible to achieve either a cant change of ±9.7°, ±1° twist with a camber factor range of 0.75 to 1.25, or the full range of twist and camber factor without any cant variation. The first option would add 24kg to the aircraft weight, whilst the second option would add around 70kg. The decision as to which of these options to choose is considered further in the trade-off section.

V. Loads Modelling

It is simply not enough to determine the best value of lift-to-drag ratio, the static and dynamic loads need to be computed for each case, as the loads relate to the structural sizing and weight, and hence drag. Results from the aerodynamic database were used to compute static bending moment distribution along the wing span, with the values at the wing-tip root, and wing root, being of particular interest. Ten cases which showed the most potential for fuel burn reduction by either increasing lift-to-drag ratio, or lowering the wing root bending moments, were selected for more detailed loads analysis. The selected cases and wing-tip properties are shown in Table 3.

The 1g loads analysis was carried out using a NASTRAN model of the full aircraft constructed from shell and beam elements, but with the fuselage, vertical tail plane and horizontal tail plane considered to be rigid. The mass of

the wings was included into the analysis directly, as the structural mass of the elements of which it is comprised, and the remaining fuselage and tail mass modelled as a lumped mass on the fuselage. The chiral wing-tip model was included in the full aircraft FE model as a beam-stick representation of the wing-tip. The beam stick model was created by using an optimizer to match its mass, static deflection and first 3 natural frequencies and mode shapes to a higher fidelity FE model of the chiral wing-tip structure.

In order to represent the aerodynamics more accurately for this aircraft model, the doublet-lattice method (DLM) used for aerodynamic loads in NASTRAN was corrected by the high-fidelity CFD data presented earlier, in order to represent the forces and moments more closely, which is particularly important considering the higher Mach numbers which are being investigated near the transonic regime. Two corrections were included into the NASTRAN aerodynamics in order that the loads on the wing match the CFD more closely, and were tuned such that the aerodynamic forces and moments are close for the range of angles of attack likely to be experienced during gust analysis. These corrections are a lift slope correction (referred to as WKK in NASTRAN) and a zero-AoA correction (referred to as W2GJ in NASTRAN).

Morphing the wing-tip has very little effect on the static inboard lift and moment distribution. The main difference is close to the wing-tip and is more noticeable as the Mach number increases. In terms of the loads there is little variation in the vertical shear, bending and twisting moments between the geometry cases, and considerable side-force and fore-aft moment variation as the wing-tip cants. This result was found across all the cases. Although the largest variations are in the side-force and fore-aft moment, these loads are still considerably smaller than the wing root bending moment, which is a key driver for the structural weight of the wing. The static wing root bending moments for the 10 cases at Mach 0.48 are shown in Figure 11. Although the exact geometry which produces the lowest wing root bending moment is different at each Mach number, the lowest cases have high cant and low twist. The fact that the optimal geometry for wing root bending moment is different at each Mach number shows that potentially loads alleviation can be achieved for varying Mach numbers.

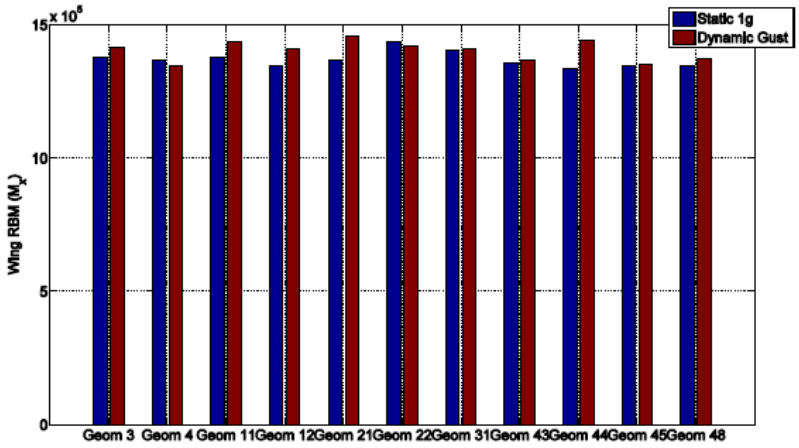

Figure 11 Comparison of the 1g wing root bending moments to the maximum dynamic gust response root bending moment at Mach 0.48

Dynamic gust computations were also performed using EASA regulation "1 – Cosine" gusts of varying length (18m – 214m) and magnitude using the $H^{1/6}$ law[22] The worst case gust length increased from 70m to 100m and 110m for Mach numbers 0.48, 0.60 and 0.74, respectively. The incremental dynamic loads are slightly higher than the 1g loads and, as the Mach number decreases, so does the difference between the two. The configurations that provide the lowest dynamic loads do not correlate with the lowest static loads cases, as seen in Figure 11. As with the 1g configuration, the lowest wing root bending moment gust response changes with Mach number, but still favors high cants. To find the optimal configuration the loads and the aerodynamic efficiency have to be taken into account and this will be discussed in the next section.

The effect of the weights for the different actuator configurations on the maximum wing root bending moments was not found to be significant. However, the mass and positioning of the actuator is much more important for the incremental wing-tip root bending moments as shown in Figure 12 where there is a noticeable change in the maximum values for different cases.

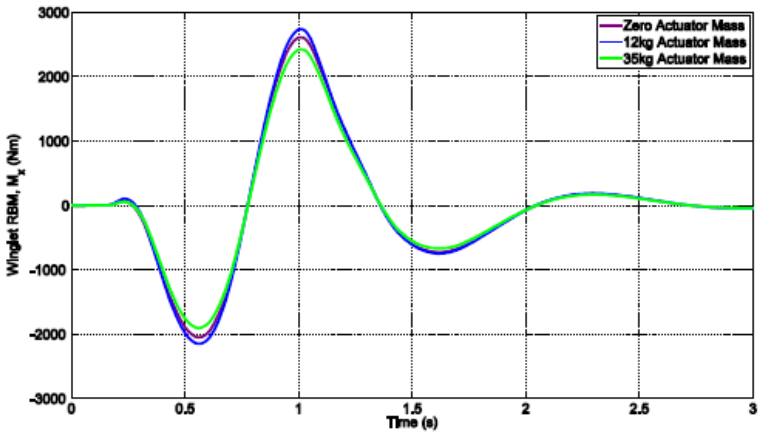

Figure 12 Wing-tip root bending time history for geometry 2, Mach 0.48, gust length 70m for various actuator layouts

VI. Trade-Off between Aerodynamic Performance and Loads

Investigation of the resulting aerodynamic performance (lift-to-drag ratio) and loads (static bending moments at the wing root and wing-tip root) shows that there is different behavior depending on the wing-tip parameters. For instance, a zero cant angle will result in reduced drag but increased bending moments, whereas a large cant angle will reduce the bending moment but increase the drag.

It is convenient to compare both parameters in terms of the well-known Breguet Range equation, such that range R is found as

$$R = \frac{V}{fg}\frac{C_L}{C_D}\ln\left(\frac{W_1}{W_2}\right) \tag{1}$$

where W_1 is the take-off weight and W_2 the landing weight. Assuming that the speed V and specific fuel consumption f remain the same, then it is possible to compare the variation of lift-to-drag ratio and the weight for the different wing-tip configurations compared to a baseline configuration, such that

W_1 = structural weight + payload + fuel + reserve fuel + ΔW

W_2 = structural weight + payload + reserve fuel + ΔW

where ΔW is the addition / reduction in weight due to an increase / decrease in bending moment on the wing and the wing-tip.

Consider a wing with cross-sectional 2nd moment of area I, then we know that the direct stress σ due to a bending moment M is

$$\sigma = \frac{My}{I} \tag{2}$$

where y is the distance from the neutral axis. If the bending moment changes by, say, p percent, then in order to maintain the same stress, the 2nd moment of area must also increase by p percent. Assuming that the chord and thickness of the wing do not change, then this increase will therefore result in an increase in weight of p% across the wing.

Taking the baseline case as 50° cant, 0° twist and a camber value of 1, then for a given mission, the comparison between the different wing-tip configurations can be defined as the fuel-mass ratio

$$S_{FM} = \frac{W_{Fuel}}{(W_{Fuel})_{baseline}} = \frac{W_1 - W_2}{(W_1 - W_2)_{baseline}} \tag{3}$$

which can be calculated from the new aerodynamics and weight assuming that the range remains constant. This function will be less than one for fuel-saving, which could also be seen as a potential of increased capable range if the same amount of starting fuel is used.

Using a neural network model to relate wing-tip configuration to the lift-to-drag ratio and wing root bending moments, an optimal wing-tip configuration is sought for least required fuel for a given mission. This optimization compares the merits of flying at a higher lift-to-drag ratio configuration against a lower wing root bending moment configuration which corresponds to an aircraft with lower structural weight.

The optimization process begins with dividing the mission into segments, at which the local optimal configuration is sought for the least amount of fuel required. A consistency check is then performed to verify mass continuity across each segment and such that the wing mass is correctly scaled to the maximum bending moment requirement of the entire mission. For each segment, the aircraft is trimmed for the rate of climb specified, with the weight of the aircraft assumed to be the averaged weight of the beginning and the end of the segment. Since only the weight of the aircraft at landing is known, the weight of the aircraft at the start of each segment is thus solved for iteratively and in reverse order from the destination.

The mission for this comparison is chosen to be a 1000km journey with maximum payload. The mission profile taken is shown in Table 4 and the aircraft is assumed to have the mass properties shown in Table 5.

Phase	Speed	Starting Altitude	Ending Altitude	Rate of Climb
Constant-Speed Climb	275kts	1500ft	5000ft	2000ft/min
Mach Climb	M0.48 to M0.74	5000ft	35000ft	1500ft/min
Cruise	M0.74	35000ft	35000ft	
Mach Descent	M0.74 to M0.48	35000ft	5000ft	-1500ft/min
Constant-Speed Descent	275kts	5000ft	1500ft	-1500ft/min

Table 4. Mission Profile

Maximum take-off mass (kg)	59000
Maximum payload (kg)	16120
Mass of aircraft at zero fuel (kg)	34407
Mass of wings (kg)	4500
Mass of wing-tip actuators (kg)	70
Mass of reserve fuel (kg)	2048

Table 5. Reference mass properties

The reserve fuel is a conservative estimate on a 45-minute loiter requirement at the landing weight, plus fuel required for initial climb, final approach and ground manoeuvers. This estimate is unchanged throughout for the optimization. For simplicity, instantaneous change of speed and climb rate as well as morphing of the wing-tip is modelled. The range of allowable morphing is 0° to 90.0° of cant, +/-5.0° of twist and camber factor of 0.0 to 2.0, with the exception of configurations where flow separation is likely to occur.

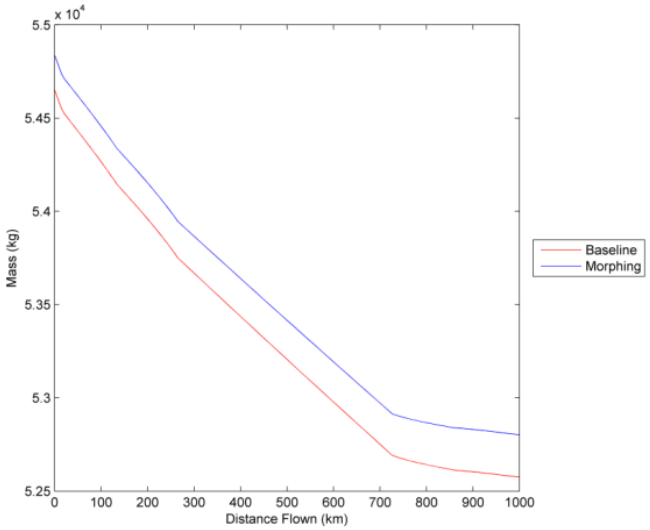

Figure 13 Mass vs. Distance Flown

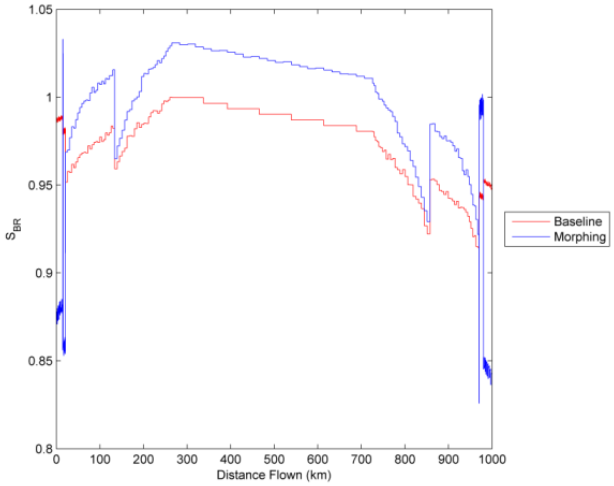

Figure 14 WRBM Ratio vs. Distance Flown

Figure 13 shows the mass of the aircraft over the mission for both the baseline and the optimized morphing configuration. The overall mass of the aircraft for the morphing-capable configuration is higher because of the additional actuators and the maximum wing root bending requirement during the flight as shown in Figure 14. Despite the wing root bending moment ratio peaking at 1.030, translating into an additional weight of 205kg for structural reinforcement, together with the addition of the actuators, the overall fuel requirement is reduced from 2077kg to 2036kg, as seen in Figure 15. This reduction gives $S_{FM} \approx 0.981$, i.e. around a 2% fuel saving.

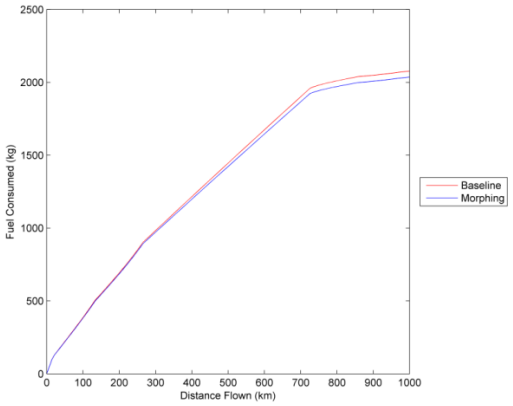

Figure 15 Fuel Consumption over Distance Flown

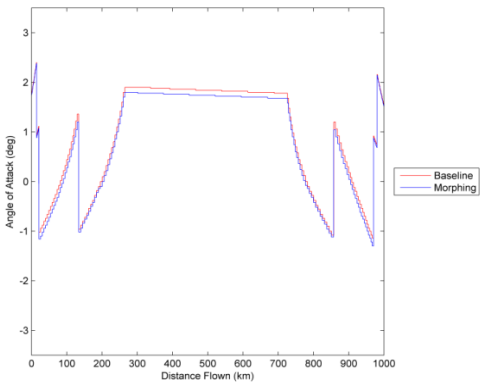

Figure 16 Angle of Attack vs. Distance Flown

Figure 16 shows that the use of morphing throughout the flight has enabled the aircraft to fly at a lower angle of attack compared to the baseline configuration, and this corresponds to increase in the lift-to-drag ratio as shown in Figure 17, which is vital for minimizing fuel usage as defined by equation (1).

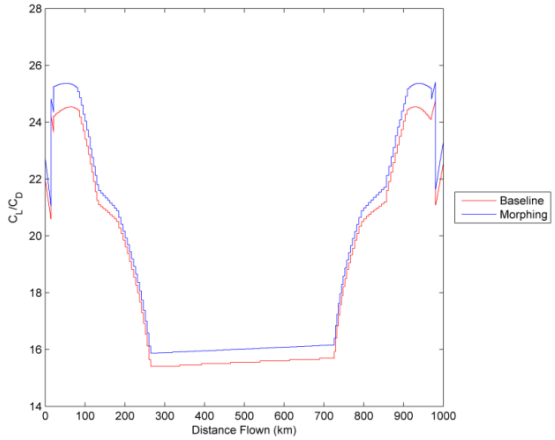

Figure 17 Lift-to-Drag Ratio vs. Distance Flown

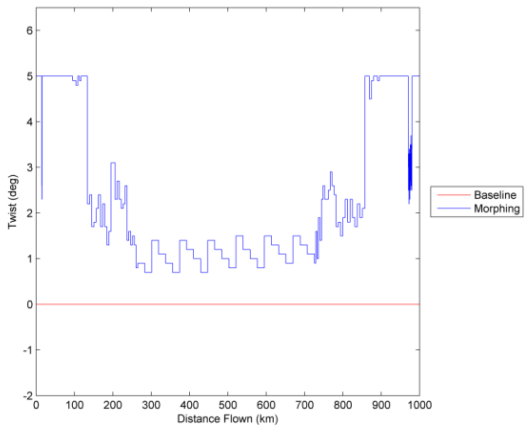

Figure 18 Wing-tip Twist vs. Distance Flown

The lift-to-drag ratio shown here may be considered higher than a typical aircraft because fuselage drag is omitted from the calculation, and also that the lift-to-drag ratio is not maximum for cruise. The lift and drag used are initially derived from a lifting-surface-only CFD computation with corrections for the drag from the tail at trimmed condition. The tail drag is calculated using Doublet-Lattice method. It is noted that the morphing concept is able to achieve superior lift-to-drag ratio over the entire mission compared to the non-morphing case.

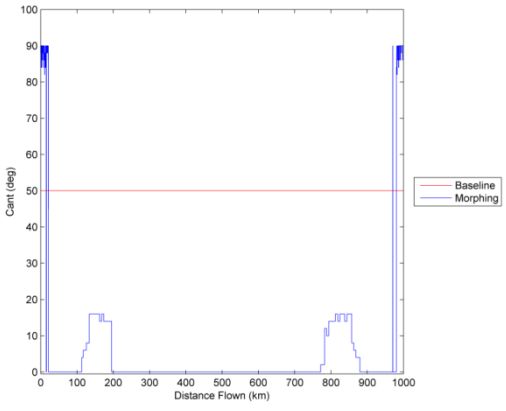

Figure 19 Wing-tip Cant vs. Distance Flown

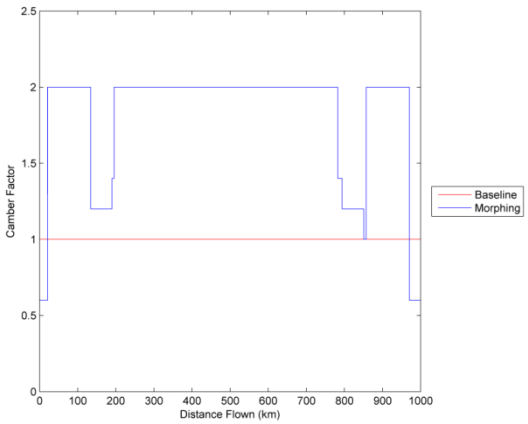

Figure 20 Wing-tip Camber Factor vs. Distance Flown

Figures 24 to 26 show the corresponding wing-tip configuration throughout the mission to achieve the minimum fuel requirement. Range of twist required for the mission vary from 1º to 5º, with most of the twist required at low altitude phase of the flight. High cant angles appear to be most favorable for the constant-speed climb and decent phase of the mission which work in conjunction with low camber. A similar trend is observed when transitioning to and from cruise.

As mentioned previously, the current actuation solutions cannot provide the full range of morphing required. Thus, the optimization was performed again, subject to the achievable range of morphing from the feasible actuation configurations. From the resulting data, it is found that using the lighter, 24kg actuation approach that allows a cant change of ±9.7°, ±1° twist with a camber factor range of 0.75 to 1.25, the possible fuel saving is reduced to around 0.67% for the same mission. The heavier 70kg option, which provides full range of twist and camber change but without cant variation, can achieve a marginally better fuel saving at approximately 0.72%.

VII. Passive Gust Loads Alleviation

A further aim of the design of the chiral wing-tip is the inclusion of a passive gust alleviation capability. Previous work[13,14] in this area has shown that if the flexural axis of a lifting surface is positioned forward of the aerodynamic center, then any effective increase in lift due to an upwards vertical gust will result in a wash-out (nose down) twist and thus there will be some reduction in the resulting gust loads. This effect will be in addition to any inherent wash-out due to the bending-torsion coupling occurring in sweptback wings. Some initial studies into the introduction of this approach for the chiral wing-tip are now described.

The leading edge region of the baseline winglet was stiffened by increasing the thickness of the front spar by 25% along with the skin in front of the spar increasing by values of 1mm through to 10mm.

The gust response of the wing was calculated for the winglet in 0° and 50° cant positions, with zero twist and a camber factor of one. Six different length 1-cosine gust responses were calculated for each configuration at Mach 0.74 at standard atmospheric conditions for 35000ft; the gust gradients were 10m, 30m, 50m, 70m, 90m and 110m. It was found that peak loads occurred for the 30m gust case. Figure 21 shows the resulting maximum wing root bending

moments (WRBMs) when the stiffening is applied to the front of the wing-tip. It can be seen that improvements between 5% and 12% in the WRBM can be achieved for all gust lengths.

Although these results have been generated separately from the aerodynamic cases, as the requirement for actuation and deflection of the chiral wing-tip is towards the rear of the airfoil section, then the inclusion of a passive gust alleviation configuration does not interfere with the adaptive aerodynamic shape optimization capability. Using the same approach as used for the previous section, the possible fuel saving is at least 3%.

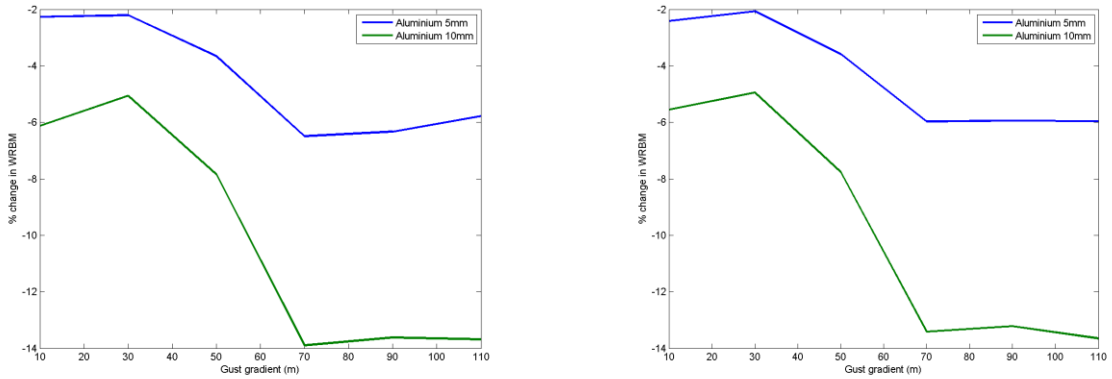

Figure 21. Percentage change in WRBM relative to the 1mm skin winglet, front 25 % stiffened. 5mm and 10mm skin thickness. Cant 0 º and cant 50 º

VIII. Conclusions

The performance of a morphing chiral wing-tip device applied to a regional jet type has been investigated. CFD computations were undertaken in order to determine the aerodynamic forces and resulting loads for a number of design test cases. Neural network surrogate models were then created using these data sets and a trade-off performed, making use of the Breguet range equation, between the improvement in lift-to-drag ratio vs. bending moment increase. It was shown that up to a 2% reduction in fuel over the reference mission could be achieved through variation of the cant, twist and camber; however, this reduction would be reduced due to current limitations in available actuators. Reductions in the gust loads of at least a further 5% were also shown possible through the implementation of a passive alleviation morphing design and this would lead to a further reductions in the fuel required for the reference mission of at least 3%.

The actuator requirements were examined and it was found that actuation of the cant, twist and camber at the same time is challenging, primarily due to space requirements. The effect of these limitations was examined and when

currently available actuators were employed in the simulation, it was found that the improvement in fuel consumption was reduced. The additional mass of the actuators does not significantly affect the morphing performance of the wing-tip.

It has been shown that it is possible to use a chiral morphing wingtip device to improve both aerodynamic performance and also develop a passive gust loads alleviation capability. The addition of extra actuation mass of the morphing wingtip was outweighed by the benefits in performance that were achieved.

Acknowledgments

The research leading to these results has received funding from the European Community's Seventh Framework Programme under the CLEAN SKY Green Regional Aircraft topic JTI-CS-2010-5-GRA-02-014: Wing loads control / alleviation system design for advanced regional Turbo-Fan A/C configuration, project number 287078. The partners in the CLAReT project are: University of Bristol, Aircraft Research Association Ltd and Stirling Dynamics Ltd.

References

[1]"European Aeronautics: A Vision for 2020". Group of Personalities. 2001, ISBN 92-894-0559-7

[2]"Flightpath 2050: Europe's Vision for Aviation", Report of the High Level Group on Aviation Research, European Commission, 2011

[3]S. Barbarino, O. Bilgen, R. M. Ajaj, M. I. Friswell and D. J. Inman, "A Review of Morphing Aircraft*", Journal of Intelligent Material Systems and Structures*, Vol. 1—January 2011

[4]J Bowman et al "Development of Next Generation Morphing Structures" AIAA-2007-1730 AIAA SDM Conf 2007

[5]*Journal of Aircraft v32 n1. Special Sec*tion : "Active Flexible Wing" 1995

[6]Pendleton E, Griffin KE, Kehoe MW & Perry B, "A Flight Test Programme for Active Aeroelastic Wing Technology" AIAA-96-1574-CP.

[7]J. Schweiger, S.,Kuzmina, A.Suleman "First results from the European research project "Active Aeroelastic Aircraft Structures", *10th AIAA/SSMO Symposium*, Albany, New York, USA, 2004.

[8]J E Cooper, A Suleman, S Ricci et al "SMorph – Smart Aircraft Structures Project" *AIAA Structures, Structural Synamics and Materials Conference*. Orlando April 2010.

[9]H. P. Monner, J. Riemenschneider, "Morphing high lift structures: Smart leading edge device and smart single slotted flap", *EC AeroDays Conference* 2011, Madrid.

[10]N.M. Ursache et al "Morphing Wing-tips for Aircraft Multi-Phase Improvement" *7th AIAA Technology, Integration and*

Operations Conf 2007.

[11]N.M. Ursache, T. Melin, A.T. Isikveren and M.I. Friswell, "Morphing Winglets for Aircraft Multi-phase Improvement" 7th *AIAA Aviation Technology, Integration and Operations Conference (ATIO*) 2007.

[12]D.D. Smith, M.H. Lowenberg, D.P. Jones and M.I. Friswell, "Computational and Experimental Validation of the Active Morphing Wing", Journal of Aircraft, Vol. 51, No. 3 (2014), pp. 925-937.

[13]D.D. Smith, R.M. Ajaj, A.T. Isikveren and M.I. Friswell, "Multi-Objective Optimization for the Multiphase Design of Active Polymorphing Wings" Journal of Aircraft, July, Vol. 49, No. 4 (2012): pp. 1153-1160

[14]L. Falcão, A.A. Gomes and A. Suleman, "Aero-structural Design Optimization of a Morphing Wingtip" Journal of Intelligent Material Systems and Structures July 2011 vol. 22 no. 10 pp 1113-1124

[15]J.E. Cooper, S. Miller, O. Sensburg, G.A. Vio, "Optimization of a Scaled Sensorcraft Model with Passive Gust Alleviation" *12th AIAA/ISSMO Multidisciplinary Analysis and Optimization* 2008,

[16]S.Miller & J.E. Cooper "Development of an Adaptive Gust Alleviation Device" *AIAA Structures, Structural Dynamics and Materials Conference* 2009. AIAA-2009-2121

[17]P Bettini , A Airoldi, G Sala, L Di-Landro, M Ruzzene and A Spadoni (2010) "Composite chiral structures for morphing airfoils: Numerical analyses and development of a manufacturing process". *Composites Part B: Engineering*, 41 (2). pp. 133 -147.

[18]D Bornengo, F Scarpa, C Remillat , "Evaluation of hexagonal chiral structure for morphing airfoil concept" *Proc IMechE, Pt G: Journal of Aerospace Engineering*, Volume 219, Number 3 / 2005 185-192

[19]A. Ruzzene and M. Spadoni, "Numerical and Experimental Analysis of the Static Compliance of Chiral Truss-ore Airfoils," *Journal of Mechanics of Materials and Structures,* pp. 965-981, 2007

[20]M. Spadoni, A. Alessandro, and A. Ruzzene. "Static Aeroelastic Response of Chiral-core Airfoils," *Journal of Intelligent Material Systems and Structures*(2007)]

[21]C. Thill, C., et al. "Morphing skins." *The Aeronautical Journal* 112.1129 (2008): 117-139

[22]J.R. Wright & J.E Cooper, "*Introduction to Aircraft Aeroelasticity and Loads*" John Wiley. 2007